



日本原子力研究開発機構機関リポジトリ
Japan Atomic Energy Agency Institutional Repository

Title	Atomistic simulation of phosphorus segregation to $\Sigma 3$ (111) symmetrical tilt grain boundary in α -iron
Author(s)	Ebihara Kenichi, Suzudo Tomoaki
Citation	Modelling and Simulation in Materials Science and Engineering, 26(6),p.065005_1-065005_10
Text Version	Accepted Manuscript
URL	https://jopss.jaea.go.jp/search/servlet/search?5062858
DOI	https://doi.org/10.1088/1361-651X/aace6a
Right	This is an author-created, un-copyedited version of an article accepted for publication/published in Modelling and Simulation in Materials Science and Engineering. IOP Publishing Ltd is not responsible for any errors or omissions in this version of the manuscript or any version derived from it. The Version of Record is available online at https://doi.org/10.1088/1361-651X/aace6a

ACCEPTED MANUSCRIPT

Atomistic Simulation of Phosphorus Segregation to $\Sigma 3$ (111) Symmetrical Tilt Grain Boundary in α -iron

To cite this article before publication: Ken-ichi Ebihara *et al* 2018 *Modelling Simul. Mater. Sci. Eng.* in press <https://doi.org/10.1088/1361-651X/aace6a>

Manuscript version: Accepted Manuscript

Accepted Manuscript is “the version of the article accepted for publication including all changes made as a result of the peer review process, and which may also include the addition to the article by IOP Publishing of a header, an article ID, a cover sheet and/or an ‘Accepted Manuscript’ watermark, but excluding any other editing, typesetting or other changes made by IOP Publishing and/or its licensors”

This Accepted Manuscript is © 2018 IOP Publishing Ltd.

During the embargo period (the 12 month period from the publication of the Version of Record of this article), the Accepted Manuscript is fully protected by copyright and cannot be reused or reposted elsewhere.

As the Version of Record of this article is going to be / has been published on a subscription basis, this Accepted Manuscript is available for reuse under a CC BY-NC-ND 3.0 licence after the 12 month embargo period.

After the embargo period, everyone is permitted to use copy and redistribute this article for non-commercial purposes only, provided that they adhere to all the terms of the licence <https://creativecommons.org/licenses/by-nc-nd/3.0>

Although reasonable endeavours have been taken to obtain all necessary permissions from third parties to include their copyrighted content within this article, their full citation and copyright line may not be present in this Accepted Manuscript version. Before using any content from this article, please refer to the Version of Record on IOPscience once published for full citation and copyright details, as permissions will likely be required. All third party content is fully copyright protected, unless specifically stated otherwise in the figure caption in the Version of Record.

View the [article online](#) for updates and enhancements.

Atomistic Simulation of Phosphorus Segregation to $\Sigma 3$ (111) Symmetrical Tilt Grain Boundary in α -iron

Ken-ichi Ebihara[‡] and Tomoaki Suzudo

Center for Computational Science & e-Systems, Japan Atomic Energy Agency
(JAEA), Tokai-mura, Naka-gun, Ibaraki 319-1195, JAPAN

E-mail: ebihara.kenichi@jaea.go.jp

Abstract. Irradiation-induced grain boundary phosphorus segregation is an important factor for estimating the embrittlement of nuclear reactor pressure vessel steels, but the physical process of phosphorus migration to grain boundaries is still unclear. We numerically studied phosphorus migration toward a $\Sigma 3(111)$ symmetrical tilt grain boundary in α -iron using molecular dynamics. We found that, in the vicinity of the grain boundary within ~ 1 nm distance, an iron-phosphorus mixed dumbbell and an octahedral interstitial phosphorus atom push a self-interstitial atom into the grain boundary, and the phosphorus atom becomes a substitutional atom. A phosphorus-vacancy complex in the region also becomes dissociated, and the vacancy is absorbed in the grain boundary without dragging phosphorus. The results claim that a novel view of the segregation process is required.

Keywords: grain boundary phosphorus segregation in iron, mixed dumbbell, octahedral interstitial phosphorus atom, phosphorus-vacancy complex, molecular dynamics simulation, first-principles calculation

[‡] Corresponding author. Tel.: +81 29 282 5976; fax: +81 29 282 6070.

1. Introduction

It is widely known that toughness reduction of steels can assist its crack propagation, and such degradation is observed when steels are cooled down from high temperatures and when they are exposed to irradiation. These effects are referred to as temper embrittlement and irradiation embrittlement, respectively [1, 2, 3, 4]. A possible mechanism of this embrittlement is the grain boundary (GB) segregation of certain kinds of elements such as tin, antimony, and phosphorus (P) that reduce the GB strength [5], being referred to as GB embrittlement [6]. Although GB segregation of solute atoms has been studied for decades [7, 8], its detailed process is still unclear; in particular, we do not know the atomistic process of how phosphorus approaches GBs and is trapped by them.

GB solute segregation is frequently measured by Auger electron spectroscopy (AES), where solute atoms are often detected within a few atomic layers from fractured GB surfaces [7], although a spread of solute atoms around a GB is also reported [9]. Meanwhile, in recent years, 3-dimensional atom probe (3DAP) has been applied to observing solutes segregated at GBs before their fracture [10, 11, 12, 13]. In such cases, solute atoms are often observed as a distribution around GBs whose full width is as large as several dozen angstroms; this is found for various kinds of solute atoms. Maruyama, et al. [13] claims, based on the observation of niobium and molybdenum in α -iron (Fe) GB, that the spatial resolution in 3DAP measurement cannot explain this broad distribution. In addition, atomic-scale simulation studies [14, 15] investigate the behavior of point defects such as vacancies and self-interstitial atoms (SIAs) around GBs and indicates the existence of a strain field around GBs. We then suspect that such a strain field

1
2
3
4
5
6
7
8
9
10
11
12
13
14
15
16
17
18
19
20
21
22
23
24
25
26
27
28
29
30
31
32
33
34
35
36
37
38
39
40
41
42
43
44
45
46
47
48
49
50
51
52
53
54
55
56
57
58
59
60

may hinder the migration of solute atoms. According to Bachhov, et al.[10], a P atoms' distribution observed at GBs in neutron-irradiated Fe-6at.%Cr alloy at 563K has the width of approximately between 30Å and 40Å for $\Sigma 5$ and large angle grain boundaries. This report implies that the GB strain field influences the migration of P atoms. In a bulk region, P atoms migrate as a mixed dumbbell, an octahedral interstitial P (octP) atom or a P-vacancy complex[16, 17, 18], but due to the strain field, the migration behaviors in the vicinity of GBs may be different.

Regarding irradiation-induced GB P segregation, some modeling studies using the rate theory is reported[19, 20], but none of them considers such strain field near GBs: In those models, P diffusion based on the first-principles calculations for the bulk region, are applied to the entire region. Besides, the models do not consider the trapping process at GBs, so that they cannot examine the influence of properties of different GBs, such as segregation energy and the amount of segregation sites, on the P segregation. Thus, if the migration behavior of P atoms in the vicinity of GBs is obtained, it is beneficial to improve such rate theory models.

For investigating atomic processes, the molecular dynamics (MD) simulation based on empirical potentials are becoming powerful methods, because the recent first-principles studies drastically improve the quality of the empirical potentials. The benefit of the method against the direct application of first-principles methods is, apparently, that the kinetics can be investigated in much larger simulation box. For example, it is reported that MD is successfully applied to studying the behavior of point defects around GBs[14, 15, 21]. Therefore, the current study also adopted this methods.

In the following, we first examine the thermal fluctuation of a $\Sigma 3(111)$ GB not

1
2
3
4
5 taking P atoms into consideration. Secondly, we study the migration of an Fe-P mixed
6 dumbbell, an octP atom, and a P-vacancy complex toward a GB using MD. The results
7 suggested that not only the thermal fluctuation of the GB but also the strain field
8 around it would become obstacles for P atoms to reach exactly on the GB, i.e., P atoms
9 truly stop migrating before they reach the GB, and the broad P distribution may not
10 be artificial but physical. This view is also reinforced by first-principles calculations.
11
12
13
14
15
16
17
18
19

20 **2. Simulation method**

21
22
23
24 We used an atomic block composed of body-centered cubic (bcc) Fe crystal holding
25 a $\langle 110 \rangle \Sigma 3(111)$ symmetrical tilt GB as the simulation box. The selected GB has the
26 smallest Σ value, so that it can be represented by a small simulation box, which is
27 also beneficial for first-principles calculations. However, it has comparatively large GB
28 energy, that is about 1.3 J/m^2 , among $\langle 110 \rangle$ symmetrical tilt GBs [22]. This means that
29 it may have a large strain field around itself. The states of a P atom at this type of GB
30 is comprehensively studied using the first-principles calculation [23]. As shown in Figure
31 1, the region of the simulation box is $42\text{\AA} \times 97\text{\AA} \times 49\text{\AA}$ and the GB is set at the center
32 in the y-direction. The number of particles in the simulation box is 14688 in most cases,
33 so that computational resources can be saved, but it is large enough to avoid defects we
34 consider going out of the box before reaching the region close to the GB. In the figure,
35 the blue particles mean Fe atoms on the regular bcc lattice site, and the white ones
36 mean the particles deviated from the regular binding state; the deviation is detected by
37 the common neighbor analysis (CNA)[24]. Both edges of the y-direction have a vacuum
38 region with about 6\AA in thickness, and the particles on the boundary surface in the x-
39
40
41
42
43
44
45
46
47
48
49
50
51
52
53
54
55
56
57
58
59
60

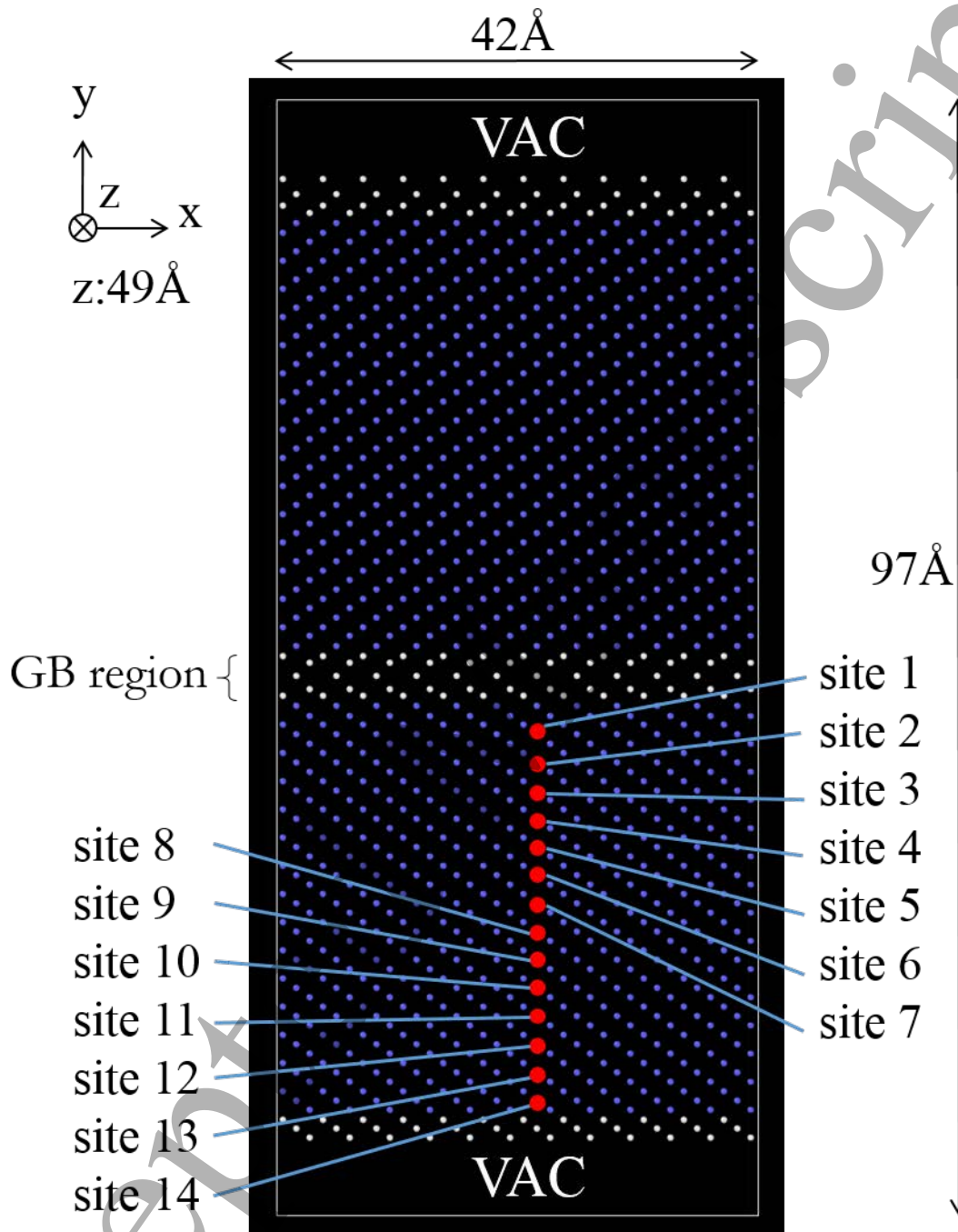


Figure 1. The bcc Fe $\Sigma 3$ (111) symmetrical tilt GB model: The red points denote initial sites for the mixed dumbbell, the P-vacancy complex, or the octP atom.

1
2
3
4
5
6
7
8
9
10
11
12
13
14
15
16
17
18
19
20
21
22
23
24
25
26
27
28
29
30
31
32
33
34
35
36
37
38
39
40
41
42
43
44
45
46
47
48
49
50
51
52
53
54
55
56
57
58
59
60

and the z-directions were fixed so that the GB cannot move to the surface of the y-direction due to thermal fluctuation. One out of an Fe-P mixed dumbbell, a P-vacancy complex, and an octP atom was inserted at one of the sites indicated by the red marks in Figure 1, and we prepared an initial state by structural relaxation. Then the P atom was tracked during the annealing simulation by an MD code LAMMPS[25] with the EAM potential proposed by Ackland et al.[26]. The adopted potential is produced by fitting to the first-principles calculation, and it is widely used and is considered as the best for a dilute P-Fe system[27]. The annealing temperature was set at 563K, being the operation temperature of pressurized water reactors and chosen also in an experimental study[10]. The time step for the numerical integration was chosen between 1 fs and 5 fs. The atomic image was visualized by using a tool called OVITO[28]. As seen in Figure 1, the GB is not a thin plane but a region with thickness, thus we refer to the region as the GB region.

3. Results

According to Figure 2, it is seen that the GB region without P atoms fluctuates thermally. Figure 3 shows the time evolution of thermal fluctuation of the GB region. According to the figure, the frequency of jumps increases as the annealing temperature increases, and the fluctuation range of the GB region is about $\pm 6\text{\AA}$ through $\pm 9\text{\AA}$ in the y-direction from the initial center of the GB region.

Figure 4 visualize the migration behavior of each defect. As seen in Figure 4(a), when a mixed dumbbell migrated and entered the region in the vicinity of the GB, that is about 12\AA from the center of the GB region, the dissociation occurred and the P atom

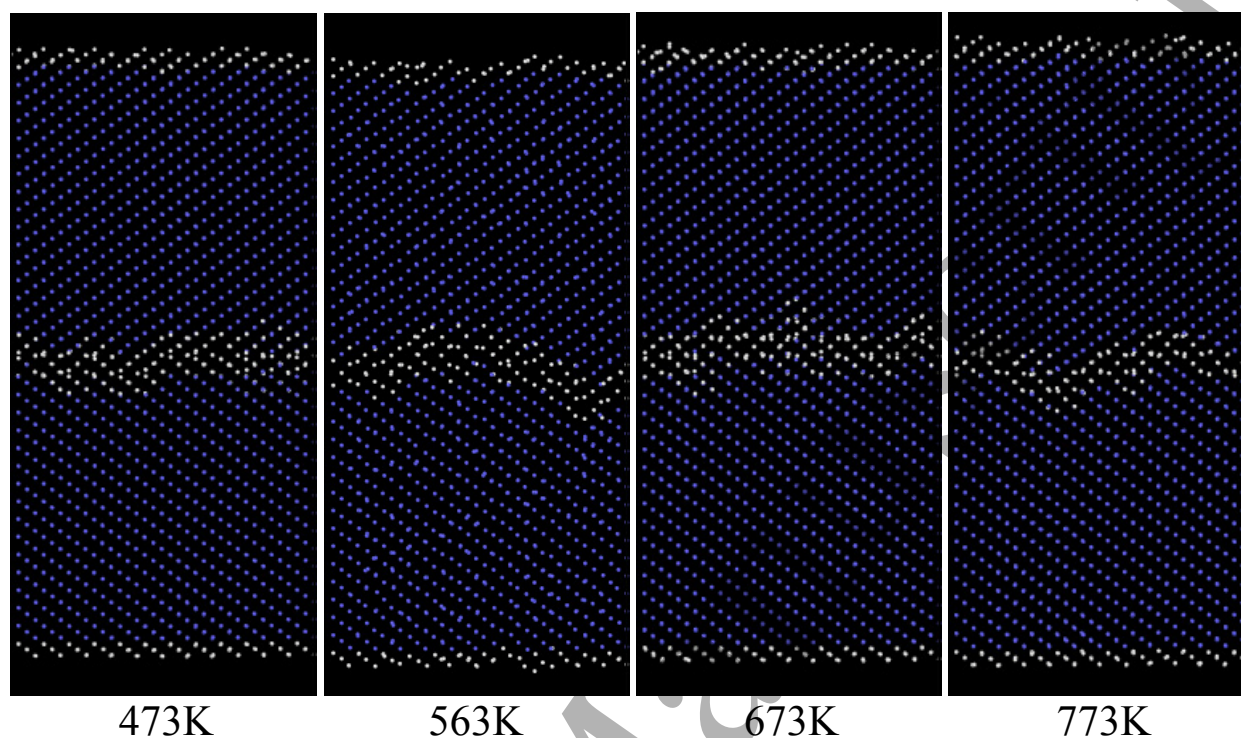


Figure 2. The snapshot of atomic configuration from 473K to 773K in the case without P atoms

became a substitutional atom and the SIA pushed an Fe atom toward the GB region. The pushed Fe atom also pushed another neighbor Fe atom and eventually an SIA was pushed into the space of the GB region. In the case of octP atoms, the situation was almost the same with the case of mixed dumbbells, in the vicinity of the GB region, the octP atom became a substitutional atom and a SIA was pushed into the GB region as shown in Figure 4(b). In the case of P-V complexes of Figure 4(c), the P-V complex migrated by the vacancy drag effect [17, 29] and it got dissociated at the point of about 15Å from the center of the GB region, the P atom became a substitutional, and the vacancy was absorbed by the GB region. The stopping behavior was observed in the vicinity not only of the GB region but of the surface for almost all of the P atoms starting from the sites shown in Figure 1. Since this phenomenon is accompanied by

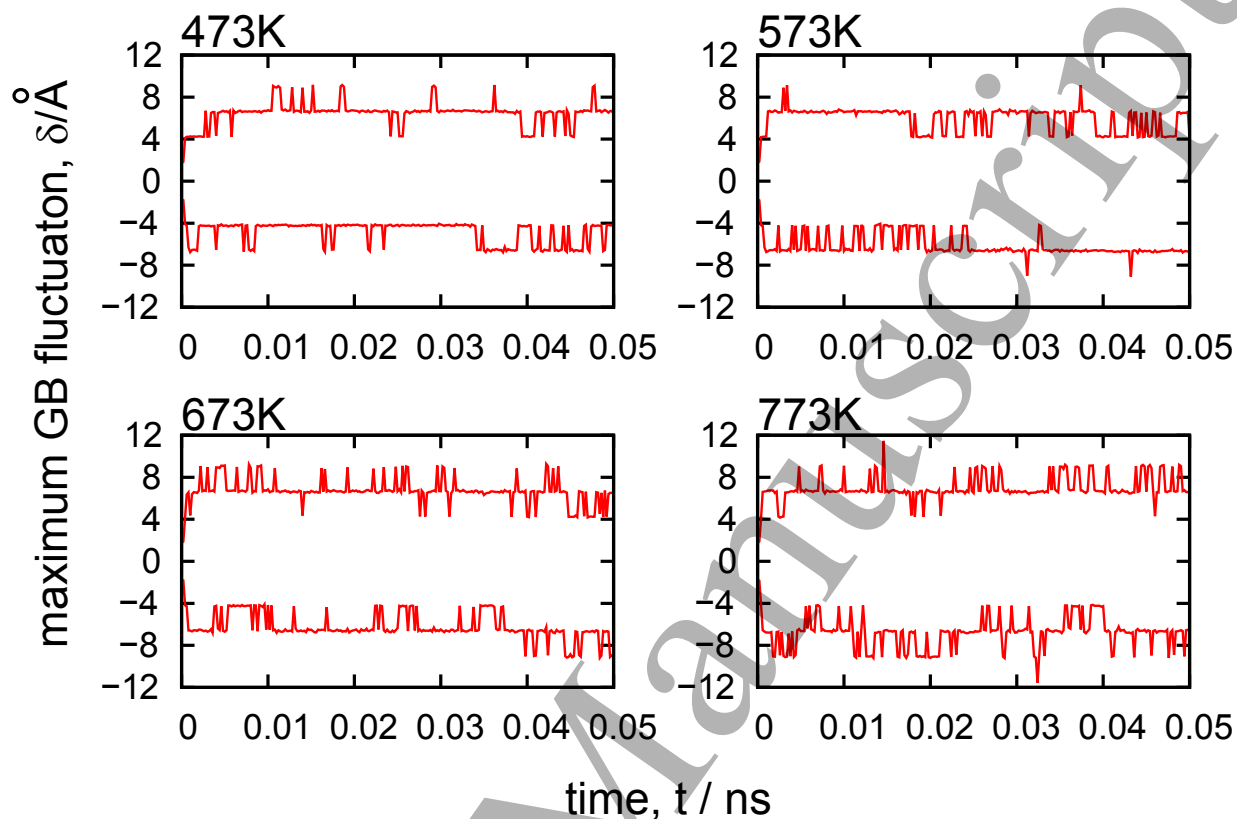


Figure 3. The thermal fluctuation of the GB region: The maximum and minimum values of the surface position of the GB region are plotted for each time step.

the absorption of SIAs or vacancies, it is considered to be dependent on the GB volume besides the strain field around the GB region. The GB volume of the adopted model is mostly as large as that of other kinds of GBs[30] and that of random GBs with high GB energy, which are often observed in practical steels, is considered to be larger than the adopted GB model. Therefore it can be considered that the current finding is not limited to the $\Sigma 3$ (111) symmetrical tilt GB.

Next, we discuss the further approach of a P atom to the GB. From the above-mentioned result, the P atom can approach the GB less than about $12\text{\AA} \sim 15\text{\AA}$ from the center of the GB region neither as a mixed dumbbell, as an octP atom nor as

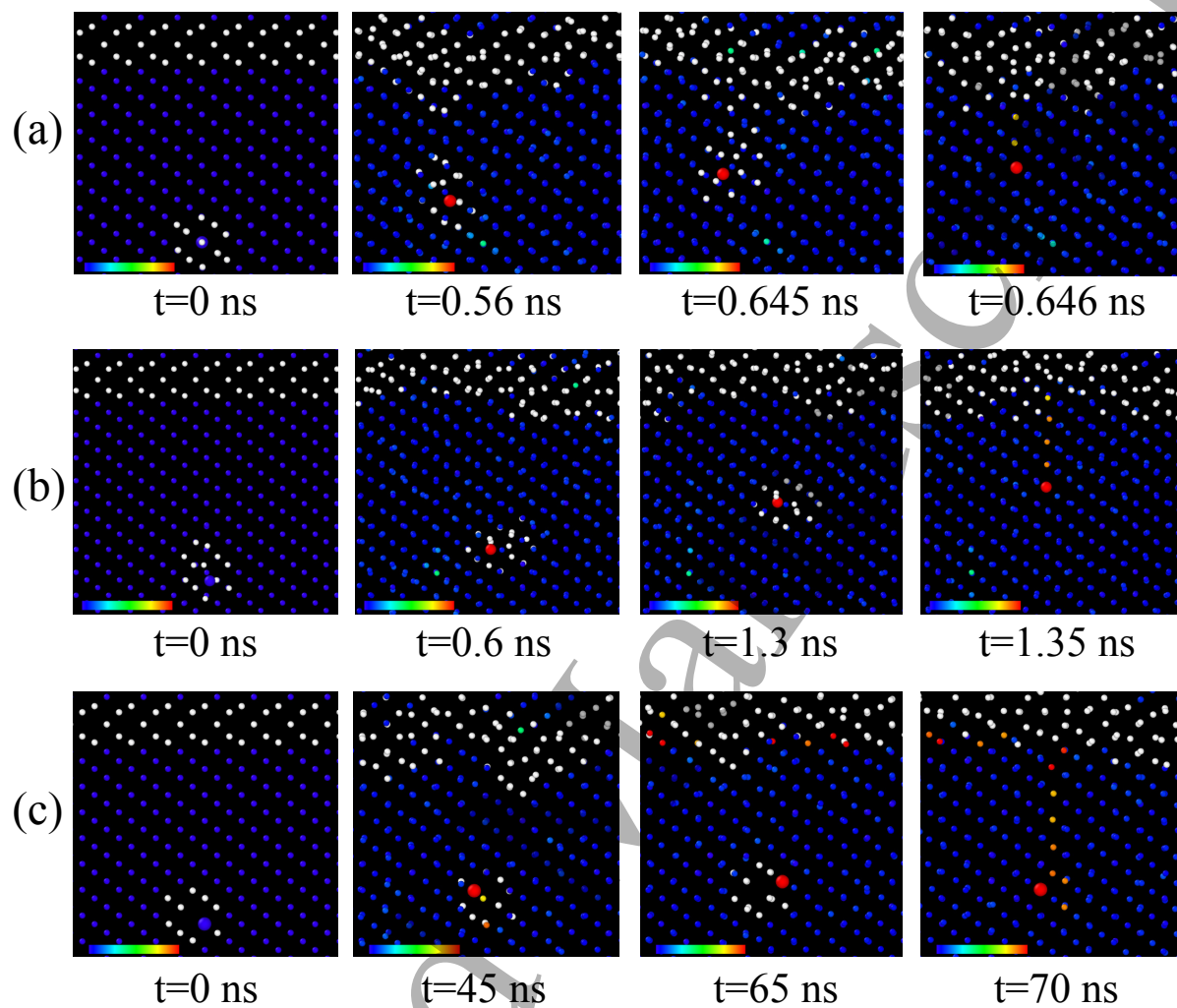


Figure 4. Migration of (a) the mixed dumbbell starting from site 7, (b) the octP atom starting from site 8, and (c) the P-V complex starting from site 7: The site number corresponds to Figures 1. The large particle is a P atom and small particles are Fe atoms. The color legend shows the displacement magnitude of particles: the red particles represent atoms which moved more than one lattice unit from their original position; the dark blue particles represent atoms staying at the original position.

1
2
3
4
5
6
7
8
9
10
11
12
13
14
15
16
17
18
19
20
21
22
23
24
25
26
27
28
29
30
31
32
33
34
35
36
37
38
39
40
41
42
43
44
45
46
47
48
49
50
51
52
53
54
55
56
57
58
59
60

10
a P-vacancy complex. This distance is too long for the GB to trap P atoms even though the thermal GB fluctuation is considered. However, P atoms are experimentally detected on the GB. This contradiction to experimental observation may be avoided if the substitutional P atom interacts with other SIAs or vacancies which come up to the 1st nearest neighbor (NN) site of the P atom. Thus, we simulated the behavior of the P atom by adding another SIA or vacancy at the 1st NN site of the P atom after the P atom becomes a substitutional atom and the dissociated SIA or vacancy is absorbed by the GB. This simulation was repeated until the P atom could no longer approach the GB. According to Figure 5, we can see that the P atom after dissociation approaches the GB gradually by successive interaction with an SIA or a vacancy. In the both cases, P atoms enter the fluctuation range of the GB, and will be absorbed by it. It is also found that the interaction with SIAs makes the P atom closer to the GB than that with vacancies. This may be because the binding energy of P atom to SIA being about 1.0eV[18] is larger than that of P atom to vacancy, which is about 0.1eV to 0.4eV[16].

4. Discussion

We conducted first-principles calculations to confirm the atomic behavior in the vicinity of the GB region which was observed in the MD calculations. For this purpose, the density functional theory (DFT) is applied in the framework of generalized gradient approximation with projector-augmented wave pseudo-potentials [31] using the Vienna ab initio simulation package (VASP) [32]. Within this framework, we adopt Perdew-Burke-Ernzerhof pseudo-potentials [33] from the VASP library. For all DFT calculations, we use a cut-off energy of 350 eV for the plane-wave basis. The supercell is composed

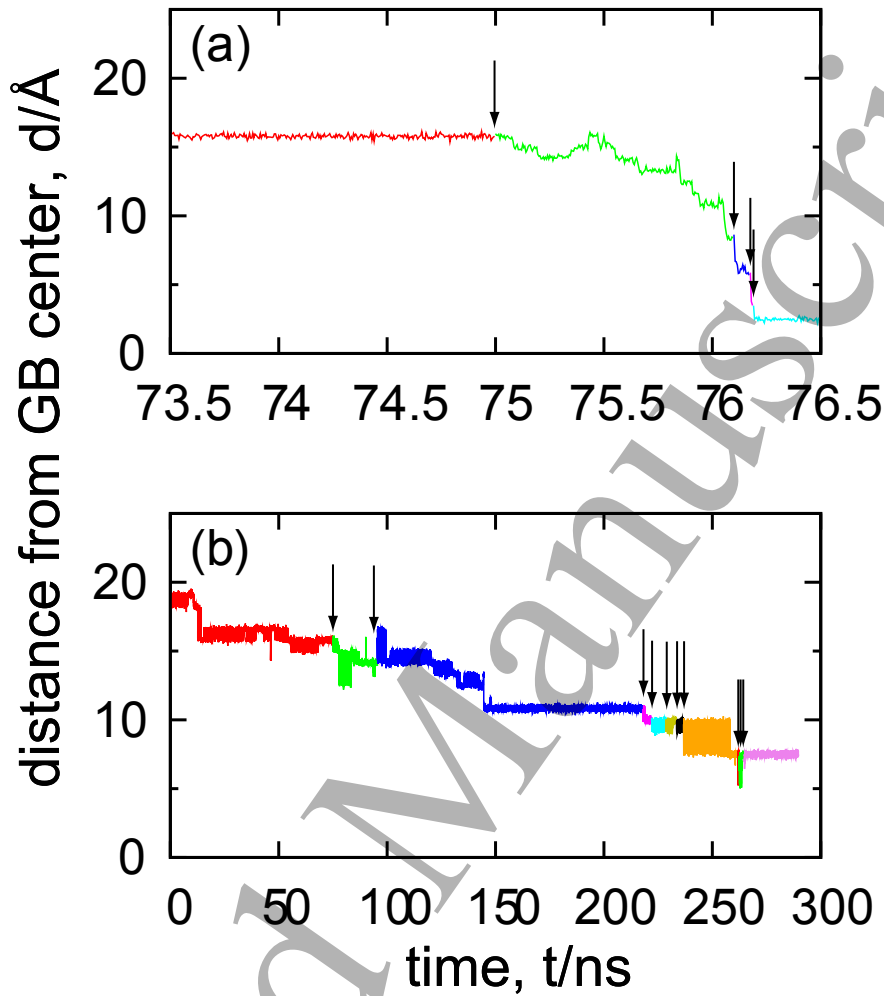


Figure 5. The behavior of the P atom by interaction with (a) SIA or (b) vacancy which is added successively at the 1st NN site of the substitutional P atom: After the P-vacancy complex starting from Site 7 in Figure 1 dissociated and the vacancy was absorbed by the GB region, an SIA or a vacancy was added. The arrow means the time when the SIA or the vacancy is added.

of 288 Fe atoms and a single phosphorus atom and includes $\Sigma 3(111)$. Monkhorst-Pack $3 \times 5 \times 1$ k-point meshes are used to sample the Brillouin zone [34]. Methfessel-Paxton smearing with 0.2 eV width is also used; the periodic boundary condition is applied to all the three directions. At first, we built a volume-relaxed supercell without P atom,

1
2
3
4
5
6
7
8
9
10
11
12
13
14
15
16
17
18
19
20
21
22
23
24
25
26
27
28
29
30
31
32
33
34
35
36
37
38
39
40
41
42
43
44
45
46
47
48
49
50
51
52
53
54
55
56
57
58
59
60

12

and set the initial condition by manually inserting specified defects. When the $\langle 111 \rangle$ mixed dumbbell was put at a site in the vicinity of the GB region as shown in Figure 6(a), the atomic rearrangement which represents an SIA pushed into a space of the GB region was seen also by the first principles calculation as shown in Figure 6(b). From this result, the behavior shown in Figure 4(a) is considered to realistically occur. In the octP and P-V complex cases, however, the absorption of an SIA or a vacancy was not confirmed by the first-principles calculations. In the octP case, it is considered that an SIA was not pushed into the GB region because the octP atom is not initially in line in the $\langle 111 \rangle$ direction with an Fe atom. However, since a migrating octP atom can easily become a mixed dumbbell, the octP's behavior in Figure 4(b) can occur in practical situations. In the P-V complex case, it is considered that the absorption of a vacancy by the GB was not observed in the first-principles calculations because there is the finite migration barrier energy even in the vicinity of the GB region. According to Bai et al.[14], its existence is shown and it is reported that its height becomes smaller in the vicinity of the GB than in the bulk region. Tschopp et al.[15] also show vacancies become easily absorbed by the GB. Thus, it is considered that the dissociation of the vacancy from the P-vacancy complex and its absorption by the GB region is likely to occur at finite temperatures.

According to the results obtained by the empirical potential, it was found that a mixed dumbbell, an octP atom, and a P-V complex cannot directly reach the GB region. In the conventional understanding of GB P segregation which is adopted in all of models using the rate theory for estimating GB P segregation[19, 20], these defects migrate in the same way with that in the bulk region and reach GBs. However, our

初期値

収束値

13

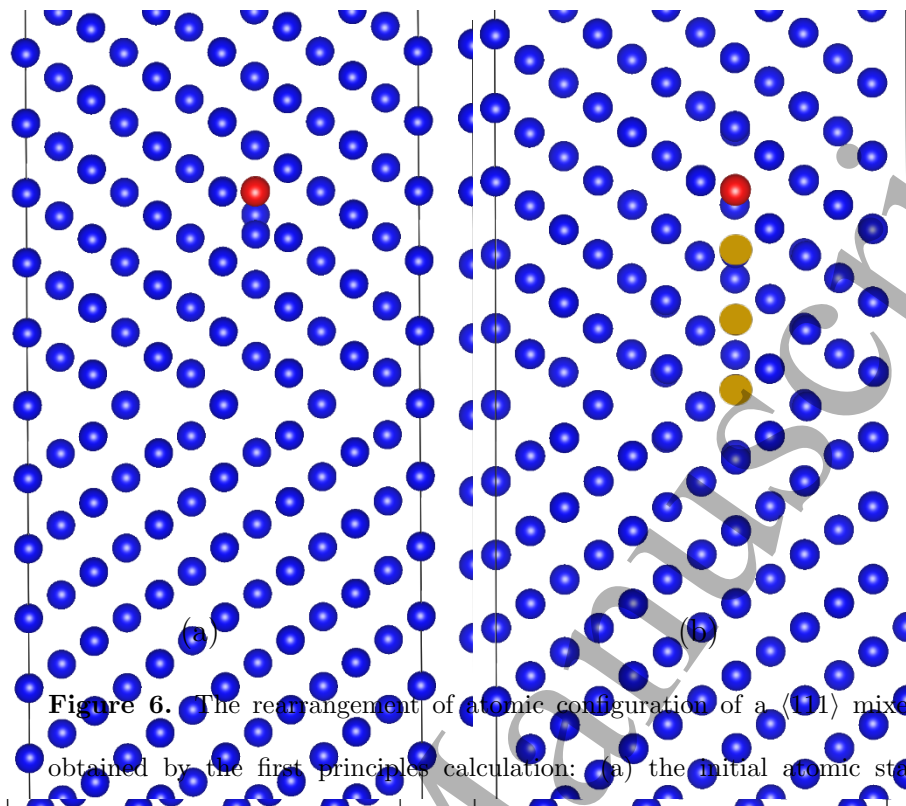


Figure 6. The rearrangement of atomic configuration of a (111) mixed dumbbell obtained by the first principles calculation: (a) the initial atomic state, (b) the atomic state after calculation convergence. In the figure, iron atoms and a P atom is represented by blue and red, respectively. In (b), the iron atom which moves largely from its initial position is represented by gold. The difference of total energy between

初期値は(111)混合ダブベル
 の初期と収束状態との差は約3.6 eV.

初期はFe、赤はP、粒子緩和後大きく移動したFeはゴールドになっている

present results suggest the necessity of revising the conventional understanding. In the modified understanding of GB P segregation, the following processes should be considered: (1) Mixed dumbbells, octP atoms, and P-V complexes migrate in the bulk region toward GBs. (2) When these defects enter the region influenced by the strain field of the GBs, P atoms of them become substitutional ones and an SIA or a vacancy becomes isolated and absorbed by the GBs. (3) The substitutional P atoms approach gradually to the GBs by successively dragged by vacancies or SIAs coming to a NN site of them. (4) The P atoms are captured by the thermally fluctuating GBs. The modified understanding can give more accurate physics of the process of segregating P atoms at GBs into the kinetic model.

In addition, it is interesting to find that the influencing range of this strain field of the GB is 30\AA in our results and is similar to the full width of P atoms' distribution around GBs in the experimental observation[10]. P atoms become substitutional atoms in the region in the vicinity of a GB and have to wait other SIAs or vacancies to migrate close to the GB center. Thus, the P behavior we found might be a possible explanation why solute atoms segregating to a GB form the broad distribution. However, such a speculation needs to be verified in the future, e.g., by longer kinetic simulations and by the experimental measurement [9].

Since the strain field of GBs can influence other kinds of solutes, the similar phenomenon might be observed besides P although there is a possibility of quantitative differences depending on the combination of GB type and solute element.

5. Conclusion

We conducted a series of MD simulations to scrutinize the P migration to a $\Sigma 3(111)$ symmetrical tilt grain boundary in α -iron. The results indicate that the strain field of GBs disturbs the migration of P atoms by stabilizing the P substitutional. This notion is also verified by first-principle calculations. It means that the migration behavior of P atoms in the vicinity of GBs is different from that in the bulk region, suggesting that a revised understanding of GB P segregation kinetics is necessary as P atoms are supposed to directly reach the GB region in the conventional understanding.

Acknowledgments

This work is supported by JSPS KAKENHI Grant Number JP15K06429.

References

- [1] McMahon C J 1968 Temper brittleness an interpretive review *Temper Embrittlement in Steel* (ASTM International)
- [2] Horn R and Ritchie R O 1978 *Metallurgical Transactions A* **9** 1039–1053
- [3] English C A, Susan O R, Gage G, Server W L and Rosinski S T 2001 Review of phosphorus segregation and intergranular embrittlement in reactor pressure vessel steels *Effects of Radiation on Materials: 20th International Symposium*
- [4] Odette G R and Lucas G E 2001 *JOM* **53** 18–25
- [5] Kameda J and McMahon C J 1981 *Metall. Trans. A* **12A** 31–37
- [6] Lejček P, Šob M and Paidar V 2017 *Prog. Mater. Sci.* **87** 83–139
- [7] Seah M P 1980 *J. Phys. F: Metal Physics* **10** 1043–1064
- [8] Harries D R and Marwick A D 1980 *Phil. Trans. R. Soc. London A* **295** 197–207
- [9] Menyhard M, Rothman B, McMahon Jr C, Lejček P and Paidar V 1991 *Acta metall. mater.* **39** 1289–1295
- [10] Bachhav M, Yao L, Odette G R and Marquis E A 2014 *J. Nucl. Mater.* **453** 334–339
- [11] Tomozawa M, Miyahara Y and Kako K 2013 *Mater. Sci. Eng. A* **578** 167–173
- [12] Jiao Z and Was G S 2011 *Acta Mater.* **59** 1220–1238
- [13] Maruyama N, Smith G D W and Cerezo A 2011 *Mater. Sci. Eng. A* **353** 126–132
- [14] Bai X M, Voter A F, Hoagland R G, Nastasi M and Uberuaga B P 2010 *Science* **327** 1631–1634
- [15] Tschopp M A, Solanki K N, Gao F, Sun X, Khaleel M A and Horstemeyer M F 2012 *Phys. Rev. B* **85** 064108–1–21
- [16] Domain C and Becquart C S 2007 *Phys. Rev. B* **75** 214109–1–8
- [17] Barashev A V 2005 *Philos. Mag.* **85** 1539–1555
- [18] Meslin E, Fu C C, Barbu A, Gao F and Willaime F 2007 *Phys. Rev. B* **75** 094303–1–8
- [19] Barashev A 2002 *Philos. Mag. Lett.* **82** 323–332
- [20] Ebihara K, Suzudo T and Yamaguchi M 2017 *Materials Transactions* **58** 26–32
- [21] Uberuaga B P, Vernon L J, Martinez E and Voter A F 2015 *Scientific Reports* **5** 9095
- [22] Shibuta Y, Takamoto S and Suzuki T 2008 *ISIJ international* **48** 1582–1591

- [23] Yamaguchi M, Nishiyama Y and Kaburaki H 2007 *Phys. Rev. B* **76** 035418–1–5
- [24] Honeycutt J D and Andersen H C 1987 *J. Phys. Chem.* **91** 4950–4963
- [25] Plimpton S 1995 *J. Comp. Phys.* **117** 1–19
- [26] Ackland G J, Mendeleev M I, Srolovitz D J, Han S and Barashev A 2004 *J. Phys., Condens. Mater.* **16** S2629–S2642
- [27] Malerba L, Marinica M C, Anento N, Björkas C, Nguyen H, Domain C, Djurabekova F, Olsson P, Nordlund K, Serra A, Terentyev D, Willaime F and Becquart C S 2010 *J. Nucl. Mater.* **406** 19–38
- [28] Stukowski A 2010 *Modelling Simul. Mater. Sci. Eng.* **18** 015012–1–7
- [29] Ebihara K, Suzudo T, Yamaguchi M and Nishiyama Y 2013 *J. Nucl. Mater.* **440** 627–632
- [30] Suzudo T and Yamaguchi M 2015 *J. Nucl. Mater.* **465** 695–701
- [31] Kresse G and Joubert D 1999 *Phys. Rev. B* **59** 1758–1775
- [32] Kresse G and Furthmüller J 1996 *Phys. Rev. B* **54** 11169–11186
- [33] Perdew J P 1996 *Phys. Rev. Lett.* **77** 3865–3868
- [34] Monkhorst H J and Pack J D 1976 *Phys. Rev. B* **13** 5188–5192